that a single, isolated phase-space hole has been shown to be unstable for all $v_d > 0$.[9] This isolated-hole instability is driven by opposing velocity gradients of $\langle f_i \rangle$ and $\langle f_e \rangle$ and is the analog to the turbulent clump instability.

Although the nonlinear instability discussed in this Letter is one dimensional and driven by velocity gradients, we believe that it is representative of an important new class of instabilities since clump and hole phenomena are predicted to occur in three dimensions with a magnetic field. For instance, it recently has been shown that a single phase-space hole in a magnetic field is unstable to a spatial density gradient.[9] This result implies that the clump instability will be driven by a spatial density gradient. Furthermore, our simulation indicates that large amplitudes are not necessary for its onset. Indeed, we have observed the instability growing out of thermal-level fluctuations.

This work is supported by the National Science Foundation and the Department of Energy. Parts of these computations were performed using MACSYMA and LISP machines at Massachusetts Institute of Technology.

[1]T. H. Dupree, C. E. Wagner, and W. M. Manheimer, Phys. Fluids 18, 1167 (1975).

[2]The calculation is for the case $\Delta x, \Delta v, > (\Delta x)_c, (\Delta v)_c$. For smaller-size windows $\langle (\delta N)^2 \rangle$ would be smaller.

[3]R. H. Berman, D. J. Tetreault, and T. H. Dupree, Bull. Am. Phys. Soc. 25, 1035 (1980), and in Proceedings of the Ninth Conference on Numerical Simulation of Plasmas, Chicago, 1980 (to be published).

[4]T. Boutros-Ghali and T. H. Dupree, to be published.

[5]T. H. Dupree, Phys. Fluids 15, 334 (1972).

[6]T. Boutros-Ghali and T. H. Dupree, Phys. Fluids 24, 1839 (1981).

[7]D. J. Tetreault, "Growth rate of the Clump Instability" (to be published).

[8]T. H. Dupree, Phys. Fluids 25, 277 (1982).

[9]T. H. Dupree, Bull. Am. Phys. Soc. 26, 1060 (1981).

Experimental Observations of Rotamak Equilibria

G. Durance,[a] B. L. Jessup,[b] I. R. Jones, and J. Tendys [a]

School of Physical Sciences, The Flinders University of South Australia, South Australia 5042, Australia

(Received 11 February 1982)

Some experimental observations of rotamak equilibria made in a high-power, short-duration (~ 80-μs) experiment and a complementary low-power, long-duration experiment are summarized. In the high-power experiment two possible equilibrium phases have been identified: an oblate, compact torus configuration and a $\beta = 1$, mirrorlike configuration. In the low-power experiment toroidal plasma current has been driven, and a compact torus configuration has been maintained, for several milliseconds.

PACS numbers: 52.55.Gb

Compact toroid configurations are currently attracting great interest because of their potential engineering advantages compared with other toroidal fusion systems. In early 1979 the proposal[1] was made that the rotating-field method of generating plasma currents[2-5] be wedded with the compact toroid approach to fusion in an apparatus which has subsequently come to be known as the rotamak.

In the rotamak concept, a rotating magnetic field is used to drive the steady toroidal current in a compact torus device. An externally applied "vertical" field couples with this toroidal plasma current to provide the inwardly directed force necessary for the equilibrium of the plasma ring. A full description of the magnetic configuration and of the experimental device can be found in Refs. 6 and 7. In the period since the publication of Refs. 6 and 7, an extensive series of current and magnetic field measurements have been made, both on a high-power, short-duration rotamak device and on a complementary, low-power, long-duration apparatus. In neither of these experiments was a steady toroidal field employed. In this Letter we present a summary of the more important observations that have been made on rotamak equilibria in these two experiments.

The high-power, short-duration experiment differed from the one described in Refs. 6 and 7 in two respects. The frequency and duration of the rotating field were 0.35 MHz and ~ 80 μsec, respectively (cf. 0.67 MHz and ~ 16 μsec), and

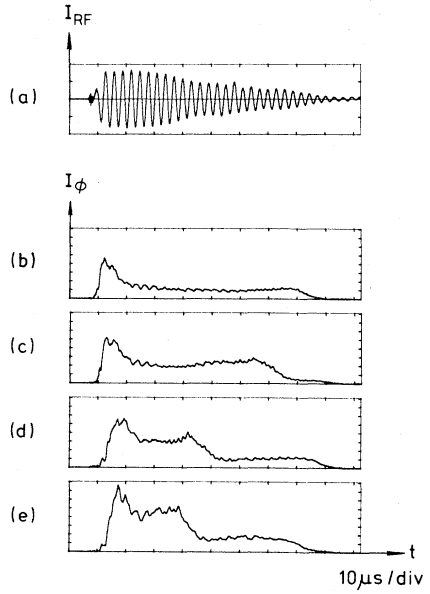

FIG. 1. (a) Characteristics of the rf pulses used to generate the rotating field; 1 kA/div. $I_\varphi(t)$ for argon filling pressure of 2.5 mTorr and applied vertical field of (b) 98 G; (c) 163 G; (d) 261 G; and (e) 327 G at $r = 0$; 2 kA/div.

the spherical Pyrex vessel was larger with an inner radius of 8.4 cm (cf. 6.4 cm). In both experiments discussed here argon was used as the working gas both to ensure that the conditions necessary for current drive were well satisfied and to take advantage of its relative ease of ionization at the low filling pressures which were used. The quantities measured were the total toroidal plasma current, I_φ, driven by the rotating field and the z component, $B_z(r,z)$, of the *total* poloidal magnetic field (i.e., the sum of the applied vertical field and the field due to I_φ). $B_z(r,z)$ was measured at a matrix of points ($\Delta r = 0.5$ cm; $\Delta z = 1$ cm) lying in the range $r = 0$ to 17 cm and $z = -6$ to $+6$ cm (the center of the discharge vessel is at $r = 0$, $z = 0$).

Figure 1 shows $I_\varphi(t)$ obtained with a filling pressure of 2.5-mTorr argon and four values of the initially imposed vertical field. The first observation is that the previously identified "steady" phase[6,7] of the rotamak discharge is maintained with apparent stability (i.e., no indication of toroidal current disruption) for times of up to 50 μsec [see Fig. 1(b)]. Secondly, a second plateau in toroidal current appears towards the end of the discharge [see Figs. 1(c)–1(e)].

In Fig. 2 the values of I_φ corresponding to the two plateau regions are plotted as a function of

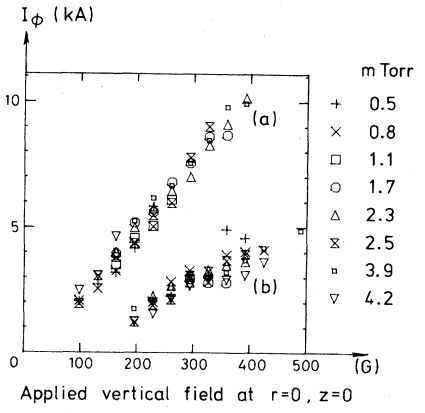

FIG. 2. I_φ vs applied vertical field at $r = 0$, $z = 0$ for (a) first current-plateau region and (b) second current-plateau region.

the value of the imposed vertical field at ($r = 0$, $z = 0$). The experimental data fall approximately on two straight lines irrespective of the filling pressure for pressures less than about 4.0-mTorr argon.

The rotamak discharge obtained for the conditions appropriate to Fig. 1(d) was studied in detail. Figure 3 shows experimentally measured contour plots of the poloidal flux function,

$$\psi(r,z) = \int_0^r r' B_z(r',z)\,dr',$$

at four different times during the discharge. Each contour differs by 400 G cm^2 from the adjacent contour. The contours were derived from a simple linear interpolation between experimental data points; no additional smoothing procedures were adopted. We believe that minor irregularities evident in the flux contours are artifacts introduced by the measurement and analysis techniques. Figure 3(c) shows the magnetic field lines of the externally applied vertical field at $t = 0$. In the initial stages of the discharge, I_φ increases to a peak value at which time Fig. 3(d) shows that the magnetic configuration is that of an oblate compact torus with the separatrix lying well outside the discharge vessel wall. The plasma must be in contact with the discharge vessel wall at this time. It is reasonable to assume that this interaction of the plasma with the wall of the vessel will cool the plasma with a consequent decrease in the number of charge carriers and an increase in the electron collision frequency. Either or both of these effects will act so as to reduce I_φ. In the experiment, it is observed that I_φ rapidly decreases until a "steady" (first current plateau)

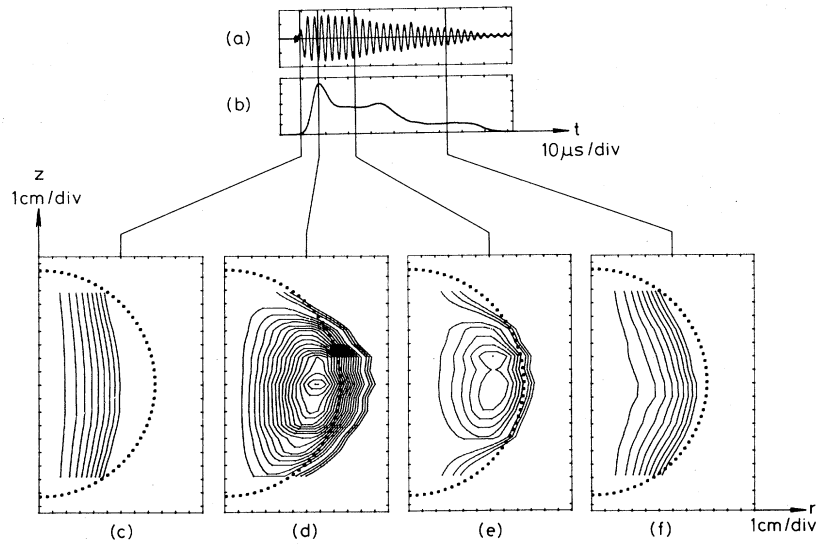

FIG. 3. (a) rf pulse, 1 kA/div; (b) filtered $I_\varphi(t)$, 2 kA/div; (c)–(f) poloidal flux contours at four times in rotamak discharge.

phase is attained. Figure 3(e) shows that the magnetic configuration obtained during this stage of the discharge is one in which the separatrix lies just at the discharge vessel wall. Measurements show that during the entire period of the first current plateau, the configuration remains symmetric; there are no evident signs of tilting. Subsequently, as the instantaneous power of the rf pulse decreases I_φ decreases to a point where it is insufficient to reverse the applied vertical field. The flux plots [Fig. 3(f)] show that a mirrorlike magnetic configuration is maintained during the entire duration of the second current-plateau phase of the discharge. Furthermore, measurements show that this configuration corresponds to a $\beta = 1$ mirror [i.e., $B_z(0,0) = 0$]. This experimental result suggests that the rotating magnetic field technique may have an application in the "end plugging" of conventional mirrors.

Bearing in mind these experimental results, obtained for one particular set of initial conditions, we surmise that all the experimental points which fall on the first current-plateau line in Fig. 2 correspond to compact torus equilibria having their separatrices lying just at the discharge vessel wall while those points which fall on the second current-plateau line correspond to $\beta = 1$ mirror configurations.

The high-power experiment described above has been complemented by a low-power, long-duration rotamak experiment in which a 6-kW rf oscillator, the output of which was appropriately divided and phase shifted, was used to generate the rotating magnetic field. The frequency, amplitude, and maximum duration of the rotating field were 0.845 MHz, 10 G, and 10 msec, respectively. The limitation imposed by the low output power was overcome by working with very low argon filling pressures. The spherical rotamak discharge vessel, of minor radius 13.5 cm, was filled with argon in the pressure range 0.1 to 0.3 mTorr. The applied vertical magnetic field in these experiments lay in the range 5 to 15 G.

Figures 4(b) and 4(c) show the $I_\varphi(t)$ and $B_z(0,0)$ oscillograms obtained in a typical discharge. For this particular experimental shot, the rotating field was pulsed on for 2.9 msec at the time of

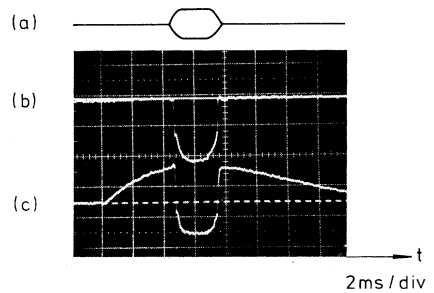

FIG. 4. (a) Schematic diagram of envelope of rotating magnetic field pulse; (b) I_φ, 138 A/div; (c) $B_Z(0,0)$, 5.8 G/div. Argon filling pressure 0.14 mTorr.

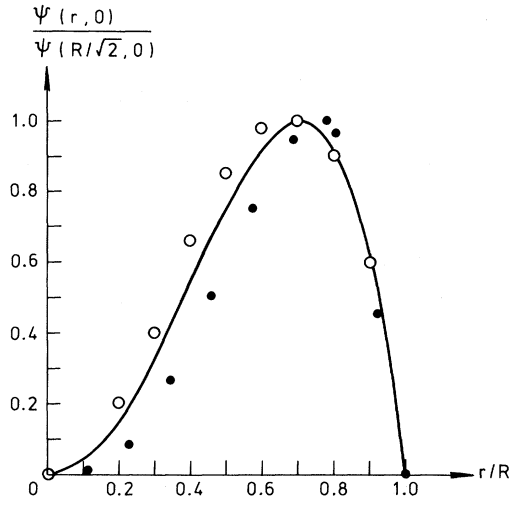

FIG. 5. $\psi(r,0)/\psi(R/\sqrt{2},0)$ vs r/R. Solid line, Solov'ev solution; closed circles, high-power short-duration experiment; open circles, low-power long-duration experiment.

maximum applied vertical field [shown schematically in Fig. 4(a)]. Figure 4(b) shows that a peak toroidal current of 280 A was driven by the rotating magnetic field. There is no indication of current disruption; the termination of the current pulse coincides with the end of the rotating field pulse. Figure 4(c) shows the initial rise of the externally applied vertical field followed by a period of field reversal brought about by the driven toroidal plasma current. Observation of the positions of the separatrix, magnetic axis, and neutral point confirmed that this period of field reversal corresponded to the generation of a compact torus configuration.

An axisymmetric toroidal equilibrium, which is an exact solution of the Grad-Shafranov equation, has been described by Solov'ev.[8] A discussion, in the rotamak context, of this solution and other classes of equilibria has been given by Storer.[9] These solutions imply a relationship between the temperature and the magnetic flux. A form of the Solov'ev solution reads

$$\psi(r,z)=\frac{r^2B_a}{2}\left[\frac{r^2}{R^2}+\frac{\alpha^2z^2}{R^2}-1\right],$$

where $B_a \equiv B_z(0,0)$, R is the position of the separatrix on the r axis, and $\alpha \equiv R/z_x$, where z_x is the position of the neutral point on the z axis. The position of the magnetic axis is at $r=R/\sqrt{2}$. It follows that

$$\frac{\psi(r,0)}{\psi(R/\sqrt{2},0)}=4\left(\frac{r}{R}\right)^2\left[1-\left(\frac{r}{R}\right)^2\right].$$

This relationship is plotted in Fig. 5 together with experimental data obtained in both the high-power (first current-plateau data) and low-power rotamak experiments described here. A reasonable fit is obtained between the Solov'ev solution and the experimental data. If now we use the Solov'ev solution to predict the plasma temperature at the magnetic axis, we arrive at the reasonable values of approximately 40 and 2 eV for the high-power and low-power experiments, respectively.

In summary, we have found the application of the rotating magnetic field technique to be a straightforward method of producing and sustaining compact toroid configurations. No evidence of instabilities has been observed in either of the two experiments described in this Letter.

We are grateful to Professor H. A. Blevin and Dr. W. N. Hugrass for many useful and stimulating discussions. This work was supported by grants from the National Energy Research, Development, and Demonstration Council of Australia, The Australian Institute of Nuclear Science and Engineering, and the Australian Research Grants Committee.

---

[a]On attachment from Research Establishment, Australian Atomic Energy Commission, Lucas Heights, N.S.W., Australia.

[b]Present address: School of Physics, University of Sydney, N.S.W., Australia.

[1]I. R. Jones, Flinders University Report No. FUPH-R-151, 1979 (unpublished).

[2]H. A. Blevin and P. C. Thonemann, Nucl. Fusion Suppl., P. 1, 55 (1962).

[3]I. R. Jones and W. N. Hugrass, J. Plasma Phys. 26, 441 (1981).

[4]W. N. Hugrass and R. C. Grimm, J. Plasma Phys. 26, 455 (1981).

[5]W. N. Hugrass, I. R. Jones, and M. G. R. Phillips, J. Plasma Phys. 26, 465 (1981).

[6]W. N. Hugrass *et al.*, Phys. Rev. Lett. 44, 1676 (1980).

[7]W. N. Hugrass, I. R. Jones, and K. F. McKenna, in Proceedings of the Third Symposium on Physics and Technology of Compact Torids in the Magnetic Fusion Energy Program, Los Alamos, 1980, Los Alamos Scientific Laboratory Report No. LA-8700-C (unpublished), p. 105.

[8]L. S. Solov'ev, *Reviews of Plasma Physics* (Consultants Bureau, New York, 1976), Vol. 6, p. 239.

[9]R. G. Storer, to be published.

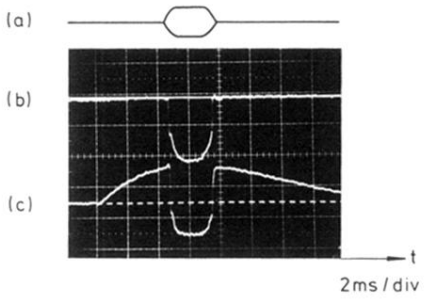

FIG. 4. (a) Schematic diagram of envelope of rotating magnetic field pulse; (b) I_{φ}, 138 A/div; (c) $B_Z(0,0)$, 5.8 G/div. Argon filling pressure 0.14 mTorr.